TITLE

A domain-general process for theta-rhythmic sampling of either environmental information or internally stored information

AUTHORS

Paul J. Cavanah[1,2,3] and Ian C. Fiebelkorn[1,2,3]

AFFILIATIONS

[1] Department of Neuroscience and Ernest J. Del Monte Institute for Neuroscience, University of Rochester, Rochester, New York, 14627

[2] Department of Brain and Cognitive Sciences, University of Rochester, Rochester, NY 14627

[3] Center for Visual Science, University of Rochester, Rochester, NY 14627

ABSTRACT

Many everyday tasks, such as shopping for groceries, require the sampling of both environmental information and internally stored information. Selective attention involves the preferential processing and sampling of behaviorally important information from the external environment, while working memory involves the preferential processing and sampling of behaviorally important, internally stored information. These essential cognitive processes share neural resources within a large-scale network that includes frontal, parietal, and sensory cortices, and these shared neural resources can lead to between-domain interactions. Previous research has linked external sampling during selective attention and internal sampling during working memory to theta-rhythmic (3–8 Hz) neural activity in higher-order (e.g., frontal cortices) and sensory regions (e.g., visual cortices). Such theta-rhythmic neural activity might help to resolve the competition for shared neural resources by isolating neural activity associated with different functions over time. Here, we used EEG and a dual-task design (i.e., a task that required both external and internal sampling) to directly compare (i) theta-dependent fluctuations in behavioral performance during external sampling with (ii) theta-dependent fluctuations in behavioral performance during internal sampling. Our findings are consistent with a domain-general, theta-rhythmic process for sampling either external information or internal information. We further demonstrate that interactions between external and internal information—specifically, when to-be-detected information matches to-be-remembered information—are not dependent on theta-band activity (i.e., theta phase). Given that these theta-independent 'match effects' occur during early processing stages (peaking at 75 ms), we propose that theta-rhythmic sampling modulates external and internal information during later processing stages.

INTRODUCTION

Completing everyday tasks, such as driving a car or shopping for groceries, often requires the sampling of both environmental information and internally stored information. The preferential processing and sampling of behaviorally important information from the external environment is broadly referred to as selective attention[1-3]. The preferential processing and sampling of behaviorally important, internally stored information is referred to as working memory[4, 5]. These essential cognitive processes involve shared neural resources within a large-scale network that includes frontal[6, 7], parietal[8-11], and sensory cortices[12-19]. While selective attention and working memory are often investigated separately, there is increasing interest in the relationship between them[16, 20-29], with shared neural resources potentially leading to between-domain interactions[22, 30-36]. Previous research has demonstrated such interactions[30], often by utilizing dual-task designs, which require both external sampling (associated with selective attention) and internal sampling (associated with working memory). This research has revealed that working memory can influence the deployment of external sampling during selective attention[31, 32, 34, 35] and vice versa[30, 37, 38]. For example, external visual targets that match to-be-remembered items in working memory can have a relative advantage over visual targets that do not match[34, 35, 39-42]. On the other hand, increasing working memory load (e.g., the number of to-be-remembered items) can decrease the detectability of near-threshold visual targets[43-45]. Given evidence for shared neural resources, some accounts have characterized working memory—or components of working memory (i.e., the sampling of temporarily stored, behaviorally important information)—as internal selective attention[21, 22, 25, 30, 46-51]. That is, there might be a domain-general process for boosting and selecting either external or internal information[16, 22, 46].

External sampling during selective attention and internal sampling during working memory are both linked to theta-rhythmic (3–8 Hz) neural activity in higher-order (e.g., prefrontal cortex) and sensory regions (e.g., visual cortex)[52-69]. Selective attention—or more specifically,

spatial attention—is sometimes compared to a spotlight that scans the visual environment, illuminating behaviorally important, external information. Whereas the classic view of this spotlight is that it can be deployed continuously, recent evidence instead indicates that it dims about 3–8 times per second[52-62]. That is, attention-related changes in neural activity and behavior performance fluctuate at a theta frequency. Recent evidence similarly shows that the strength of neural representations associated with behaviorally important, internally stored information fluctuates at a theta frequency (i.e., during working memory)[63-69]. Such theta-rhythmic sampling of external and internal information might help to resolve the competition for overlapping neural resources by isolating neural activity associated with different functions (or representations) over time[52]. For example, in the context of external sampling, theta-rhythmic sampling seems to coordinate sampling (i.e., sensory functions) and shifting (i.e., motor functions) within the brain regions that direct both selective attention and goal-directed orienting movements (i.e., the 'Attention Network')[56, 70, 71].

Given that (i) the enhancement of behaviorally important information and external sampling during selective attention and (ii) the maintenance of behaviorally important information and internal sampling during working memory rely, at least in part, on shared neural resources[17, 72-75], a competition between these processes might be resolved by alternately biasing neural resources toward one function or the other (i.e., over time). Balestrieri, Ronconi and Melcher [45] recently used a dual-task design and behavioral data to provide evidence of an interaction between selective attention and working memory during external sampling. The frequency of external sampling (i.e., fluctuations in the detection of a near-threshold visual target) slowed with increasing working memory load (i.e., from ~7.5 Hz to ~5 Hz), indicating that neural processes associated with working memory can influence the temporal dynamics of external sampling. Here, we used electroencephalography (EEG) and a dual-task design to directly compare (i) theta-dependent fluctuations in behavioral performance during external sampling with (ii) theta-dependent fluctuations in behavioral performance during internal

sampling. We specifically compared the relationship between the phase of theta-band activity and behavioral performance on trials that probed either external sampling (i.e., with a noise-added visual target) or internal sampling (i.e., by retro-cueing a to-be-remembered item). That is, we first tested whether there is a domain-general, theta-rhythmic process for sampling either external information or internal information. We then tested whether behavioral and electrophysiological interactions that occur when external information matches internal information[31, 32] (i.e., so-called 'match effects') are dependent on the phase of theta-band activity (i.e., are modulated by theta-rhythmic sampling). These further analyses provided clues as to where in the processing hierarchy theta-rhythmic sampling is influencing the selection of external and internal information (and subsequently behavioral performance).

RESULTS

Here, we examined behavioral and electrophysiological measures during an experimental task (Fig. 1A) that required only external sampling, only internal sampling, or both external and internal sampling (i.e., dual-task trials). Participants (n = 25) maintained fixation throughout the duration of each trial and indicated, following a variable delay (0.3–2.5 seconds), whether a pre-cued visual target (i.e., 'external-probed trials') or a retro-cued memory item (i.e., 'internal-probed trials') was either a horizontal grating or a vertical grating. On dual-task trials, either visual targets or retro-cues occurred with equal probability (i.e., participants could not anticipate whether external sampling or internal sampling would be probed following the variable delay). Dual-task trials included three subtypes: (i) external and internal sampling at the same location (i.e., 'both, 1L same'), (ii) external and internal sampling at different locations (i.e., 'both, 1L diff'), and (iii) external and internal sampling at the same two locations (i.e., 'both, 2L same'). To promote the deployment of selective attention in anticipation of visual targets, we added noise to the visual gratings (Fig. 1A), pinning each subject's accuracy on external-only trials at approximately 80 percent. In comparison, accuracy on external-probed dual-task trials was

allowed to vary from 80 percent (i.e., to measure changes in behavioral performance associated with dual-task trials). Memory items—presented prior to the variable delay—were noiseless visual gratings.

Figure 1B compares behavioral performance on external- and internal-only trials (i.e., 'alone' trials) to behavioral performance on dual-task trials, collapsed across trial subtypes (i.e., collapsed across the 'both, 1L same', 'both 1L diff', and 'both, 2L same' conditions). Supplemental Figure 1 shows behavioral performance separately for each subtype of the dual-task conditions. For accuracy, a repeated measures ANOVA revealed main effects of both trial type (i.e., alone trials vs. dual-task trials; $F = 5.14$ and $p = 0.0326$) and probe type (i.e., external probe vs. internal probe; $F = 47.47$ and $p = < 0.0001$). Although dual-task trials were associated with an apparent decrease in accuracy for external-probed trials—but not for internal-probed trials (Fig. 1B)—the interaction between trial type and probe type did not reach statistical significance ($F = 3.64$ and $p = 0.0682$). For response times (RTs), a repeated measures ANOVA revealed no significant main effects for either trial type ($F = 0.01$ and $p = 0.9038$) or probe type ($F = 2.6448$ and $p = 0.1169$); however, there was a significant interaction between trial type and probe type ($F = 29.32$ and $p < 0.0001$). Follow-up t-tests revealed a significant difference in RTs between external- and internal-probed dual-task trials ($p = 0.0349$), with no such difference in RTs for alone trials ($p = 0.9635$). That is, participants were significantly slower to respond on dual-task trials with an external probe (i.e., a noise-added grating) than dual-task trials with an internal probe (i.e., a retro-cue).

The primary purpose of this study was to investigate whether there is a common, theta-rhythmic process for sampling external information (during selective attention) and internally stored information (during working memory). We first calculated phase-behavior relationships for all external-probed trials and all internal-probed trials (Fig. 2). Here, we used wavelets to measure frequency-specific phase during the variable delay, just prior to either a visual target (i.e., external-probed trials) or a retro-cue (i.e., internal-probed trials)[56, 63, 76, 77]. Because

accuracy on internal-probed trials was near ceiling, we focused on the relationship between frequency-specific phase (from 3–55 Hz) and RTs (but see later analyses showing that accuracy for external-probed trials also fluctuates as a function theta phase, Fig. 5B). After obtaining phase measurements for each trial at each electrode, we calculated median RTs in overlapping phase bins (i.e., we measured RTs has a function of phase, see Fig. 2D). We then fit the phase-RT functions with a one-cycle sine wave and used the amplitude of that sine wave to measure the strength of the phase-RT relationships (after averaging the phase-RT functions across participants)[56, 63, 76, 77]. This approach is based on the assumption that there will be a phase associated with relatively better behavioral performance, and 180 degrees from that phase, a phase associated with relatively worse behavioral performance[56, 76]. Figure 2A shows the strength of the phase-RT relationships for every electrode (1–128) and frequency (3–55 Hz) combination, separately for external- and internal-probed trials. Here, we zeroed statistically insignificant results, after using a non-parametric permutation approach and cluster-based statistics (i.e., to correct for multiple comparisons)[78]. Supplemental Figure 2B shows the non-zeroed results. The frequencies and electrodes associated with significant phase-RT relationships ($p < 0.05$) are strikingly similar across external- and internal-probed trials (Fig. 2A), with significant phase-RT relationships primarily occurring in the theta- and alpha-frequency bands, peaking at 4–5 Hz and 9–11 Hz (Fig. 2B). Figure 2C shows the clusters of electrodes with significant phase-RT relationships and the associated topographies at 4 Hz and 9 Hz. Because the likelihood of microsaccades has also been shown to fluctuate as a function of theta phase[79], we re-calculated our results after excluding trials with microsaccades occurring during the delay. Supplemental Figure 2A, consistent with previous research[56, 58], shows that the pattern of phase-RT relationships is similar with and without microsaccades, indicating that phase-RT relationships are not attributable to microsaccades.

In addition to examining whether significant phase-RT relationships for external and internal sampling occurred at similar electrodes and frequencies, we measured whether faster

and slower RTs for external and internal sampling were associated with similar phases[63]. Here, we used phase-RT functions from a single electrode, taken from the frontal cluster (i.e., the electrode with the strongest phase-RT relationship). As shown in Figure 2D, the phases associated with faster and slower RTs, at 4Hz, were consistent for external- and internal-probed trials. We used a circular Watson-Williams test[63, 80] to statistically test whether the specific phase associated with faster RTs differed between external- and internal-probed trials. This test demonstrated that the distributions of fast-RT phases (across participants) for external- and internal-probed trials were not statistically different between these conditions ($p = 0.2435$). Figure 2E shows the circular histograms associated with fast-RT phases for external- and internal-probed trials ($n = 25$).

Figure 3 shows phase-RT relationships for external- and internal-probed trials, separately for alone trials and each subtype of the dual-task conditions (i.e., 'both, 1L same', 'both, 1L diff', and 'both, 2L same'). Here, we show these relationships at 4 Hz; Supplemental Figure 3 shows the same phase-RT relationships at 9 Hz. While the significant electrode clusters vary across these conditions, the topographies (Fig. 3A) and the specific phases (Fig. 3B) associated with faster and slower RTs are similar. That is, the results are largely similar for external- and internal-probed trials, regardless of whether trials required only external sampling, only internal sampling, or both external and internal sampling. We again used a circular Watson-Williams test[63, 80] to statistically test whether the specific phase associated with faster RTs differed between external- and internal-probed trials. This test demonstrated that the distributions of fast-RT phases (across participants) for external- and internal-probed trials were not statistically different between these trial types for 'alone' trials ($p = 0.5121$), 'both, 1L same' trials ($p = 0.9934$), 'both, 1L diff' trials ($p = 0.0798$), or 'both, 2L same' trials ($p = 0.1650$). Rather than being coordinated at different phases of theta-band activity, the present results (Figs. 2 and 3) are consistent with a shared theta-rhythmic process (i.e., a domain-general process) for sampling either environmental information or internally stored information. A closer look at

Figure 3B suggests that effect sizes (i.e., the strength of the phase-RT relationships) were lower for the dual-trial conditions where environmental information and internally stored information were associated with the same spatial locations (i.e., the 'both, 1L same' and the 'both, 2L same' trials). See the Discussion section for further interpretation of this observation.

After comparing relationships between frequency-specific phase and behavioral performance for external and internal sampling, we next investigated behavioral and electrophysiological interactions between (i) the enhancement of behaviorally important information and external sampling during selective attention and (ii) the maintenance of behaviorally important information and internal sampling during working memory. Here, we binned external-probed, dual-task trials based on whether the to-be-detected information (i.e., the target) was a 'match' or a 'non-match' for the to-be-remembered information (i.e., a memory item). For the 'both, 1L same' condition and the 'both, 2L same' conditions (see Fig. 4A), a match was defined by both the orientation and the spatial location of the gratings (i.e., the matching information occurred at the same location in space). For the 'both, 1L diff' condition (see Fig. 4A), however, a match was only defined by the orientation of the gratings (i.e., the external and internal information for this condition always occurred at different spatial locations). Previous research has shown that interactions between external and internal information change over time[31], we therefore split our trials based on the median delay (i.e., 1.4 seconds) into short-delay trials and long-delay trials. Figure 4B shows accuracy for the different dual-task conditions, separately for 'match' and 'non-match' trials. We conducted repeated measures ANOVAs to test for behavioral effects. Short-delay trials we associated with significant main effects of condition ($F = 5.29$ and $p = 0.0084$) and match status ($F = 5.98$ and $p = 0.0222$) and a significant interaction between condition and match status ($F = 4.48$ and $p = 0.0165$). Follow-up t-tests revealed significantly different accuracy for 'match' and 'non-match' trials from the 'both, 1L same' ($p = 0.0410$) and the 'both, 2L same' conditions ($p = 0.0365$), but no corresponding difference in accuracy for the 'both, 1L diff' condition ($p = 0.8013$). Matching information on

short-delay, external-probed trials led to worse accuracy, but only when the external and internal information were a match for both orientation and spatial location (i.e., there were no match effects for the 'both, 1L diff' condition, when external and internal information were presented at different spatial locations). In comparison, long-delay trials were not associated with significant main effects of either condition ($F = 0.24$ and $p = 0.7887$) or match status ($F = 0.42$ and $p = 0.5229$), nor were they associated with a significant interaction between condition and match status ($F = 0.09$ and $p = 0.9073$). To better visualize the temporal dynamics of behavioral interactions between external and internal information (Fig. 4C), we also calculated accuracy for 'match' and 'non-match' trials in overlapping delay bins (600-ms bins, with a step size of 10 ms). Here, we restricted our analysis to the conditions previously associated with match effects (i.e., we combined data from the 'both 1L, same' and the 'both 2L, same' conditions). Figure 4C confirms that match effects decrease over time, persisting slightly beyond the median delay (i.e., beyond 1.4 seconds).

To test for electrophysiological interactions between external and internal sampling, we calculated event-related potentials (ERPs), time-locked to the external probe (i.e., the noise-added grating), separately for 'match' and 'non-match' trials. Again, we restricted our analysis to the conditions previously associated with match effects (i.e., we combined data from the 'both 1L, same' and the 'both 2L, same' conditions, see Fig. 4B). Figure 4D shows a cluster of electrodes with a significant difference ($p < 0.05$) between the ERPs for 'match' and 'non-match' trials (Fig. 4E). These 'match effects' occurred during short-delay trials but not during long-delay trials, consistent with the behavioral findings (Fig. 4B). Moreover, these match effects peaked at 75 ms (time-locked to the probe), within the timeframe of the earliest, feedforward sensory components[81].

Finally, we repeated the same comparisons between 'match' and 'non-match' trials (Fig. 4A), after first sorting trials into two bins based on theta phase (at 4Hz): a 180-degree bin centered on the 'good' theta phase (i.e., the phase associated with relatively better behavioral

performance) and a 180-degree bin centered on the 'bad' theta phase (i.e., the phase associated with relatively worse behavioral performance). That is, we tested whether match effects in behavioral performance and ERPs were dependent on theta phase (i.e., theta-rhythmic sampling). Again, we combined data from the 'both 1L, same' and the 'both 2L, same' conditions (i.e., the conditions that previously demonstrated significant match effects in behavioral performance, see Fig. 4B). We further restricted our analysis to short delay-trials (delay < 1.4 seconds), where we previously observed significant match effects (Fig. 4B). It should be noted that even after combining trials across conditions, trial counts for these analyses were low (i.e., the mean was 29.4 trials per subject/condition). A repeated measures ANOVA demonstrated significant main effects of theta phase ($F = 8.75$ and $p < 0.0069$) and match status ($F = 10.57$ and $p = 0.0034$) on accuracy, but indicated the absence of an interaction between theta phase and match status ($F = 0.01$ and $p < 0.9112$). While theta phase was associated with fluctuations in accuracy (for external-probed, dual-task trials), it did not influence match effects (i.e., differences in accuracy across 'match' and 'non-match' trials) (Figure 5A). Similarly, although there were no significant effects in the theta-binned ERPs (likely due to low trial counts), early match effects in the ERPs looked similar across the 'good' and 'bad' theta-phase bins. Theta phase was therefore generally associated with fluctuations in behavioral performance, but it did not modulate behavioral or electrophysiological interactions between external and internal sampling (i.e., interactions that occur when to-be-detected information matches to-be-remembered information).

DISCUSSION

Both selective attention and working memory involve the sampling of information, either environmental information (during selective attention) or internally stored information (during working memory). Recent evidence suggests that this sampling, whether turned outward[52-62] or inward[66, 68], fluctuates at a theta frequency (3–8 Hz). In the context of selective attention,

attention-related behavioral and neural effects wax and wane as a function of theta phase[52-62]. We have proposed that these temporal dynamics reflect alternating attentional states associated with either sampling (i.e., sensory functions of the large-scale network that directs selective attention) or a greater likelihood of shifting (i.e., motor functions of the large-scale network that directs selective attention)[52, 53, 56]. These alternating attentional states[56, 77] might help to resolve *functional* conflicts attributable to shared neural resources. In the context of working memory, theta-rhythmic neural activity might also, for example, help to resolve *representational* conflicts attributable to shared neural resources. Specifically, previous work has shown that the strength of neural representations associated with to-be-remembered items waxes and wanes as a function of theta phase[63-68] (or theta-dependent, higher frequency phase[63, 64]), with different to-be-remembered items being associated with different phases (i.e., there is a phase-specific coding of different items). In other words, whether a task involves the sampling of environmental information or the sampling of internally stored information, the selection and/or enhancement of behaviorally important information fluctuates at a theta frequency.

Previous work has separately investigated theta-rhythmic sampling during selective attention and theta-rhythmic sampling during working memory. Here, we investigated whether there is a domain-general sampling process. That is, we investigated whether theta-rhythmic sampling during selective attention and theta-rhythmic sampling during working memory shared a neural basis. We therefore compared evidence of theta-rhythmic sampling across trials that required (i) only external sampling, (ii) only internal sampling, or (iii) both external and internal sampling (i.e., dual-task trials). Here, theta phase prior to the onset of either a visual target (i.e., during external-probe trials) or a retro-cue (i.e., during internal-probe trials) was linked to similar fluctuations in behavioral performance (Figs. 2 and 3), regardless of whether there was a potential conflict between external and internal sampling (i.e., during dual-task trials) or not (i.e., during only-external trials or only-internal trials). Both the topographies of behaviorally relevant

theta-band activity (i.e., phase-RT relationships) and the specific theta phases associated with either better or worse behavioral performance were similar across trials that probed external sampling and trials that probed internal sampling (Figs. 2 and 3). The present findings are therefore consistent with a domain-general, theta-rhythmic process for sampling either environmental information or internally stored information. Given the spatial limitations of the EEG signal (attributable to volume conduction), future research—using methods with greater spatial resolution (e.g., neurophysiology in non-human primates)[16, 46, 82]—will need to address whether this domain-general process (i) can concurrently sample external and internal information, perhaps by interacting with domain-specific neural populations[16, 82], or (ii) alternates between periods of sampling external information and periods of sampling internal information. To clarify the second alternative, it may be that the domain-general process for theta-rhythmic sampling can either be turned inward or outward at any given moment in time (but not concurrently inward and outward). Whether external sampling and internal sampling are concurrent or isolated over time might change depending on the degree of representational overlap (i.e., the degree of similarity between environmental information and internally stored information). Our findings (see Fig. 3B), for example, suggest that phase-RT relationships were weaker when external and internal sampling involved the same spatial locations (i.e., for 'both, 1L same' trials and 'both, 2L same' trials). Increased overlap in the neural populations representing environmental and internally stored information (i.e., an increased competition between internal and external sampling for limited processing resources) might necessitate that these processes become isolated over time, leading to overall weaker phase-RT relationships. That is, as a result of these processes being isolated over time, (i) periods when theta phase is more strongly related to behavioral performance on external-probed, dual-task trials might alternate with (ii) periods when theta phase is more strongly related to behavioral performance on internal-probed, dual-task trials.

Future research will also need to test whether there is a specific theta phase associated with a higher likelihood of shifts between periods of external and internal sampling. Although between-domain shifts (e.g., from external to internal) have yet to be examined in the context of theta-rhythmic sampling, previous work has provided evidence that within-domain shifts (e.g., attentional shifts between different locations in the environment) occur at a consistent theta phase[52, 60, 70, 83]. Evidence for or against a common mechanism for shifting within or between domains is mixed. Most research has separately investigated shifting within the contexts of either external sampling[1] or internal sampling[47] (i.e., focusing exclusively on within-domain shifts). Recent research, however, has shown (i) that between-domain shifts lead to greater behavioral (or switch) costs than within-domain shifts[84, 85], and (ii) that a multivariate classifier can discriminate within- from between-domain shifts[85]. These findings suggest at least partly distinct underlying neural processes. In contrast, the same research demonstrated that changes in alpha lateralization attributable to within- and between-domain shifts have equivalent time courses[85]. Alpha lateralization is associated with spatial orienting[86], and equivalent time courses for changes in alpha lateralization (i.e., when the to-be-sampled information shifts from one visual hemifield to the other) provide evidence that within- and between-domain shifts have equivalent time courses. Based on evidence from the present experiment (Figs. 2 and 3) of a domain-general, theta-rhythmic process for sampling either external or internal information, we predict that the likelihood of between-domain shifts—like within-domain shifts[52, 60, 70, 83]—fluctuates as a function of theta phase.

While we have thus far focused on the relationship between theta phase and behavioral performance (peaking at 4–5 Hz), phase-RT relationships in the present experiment spanned lower frequencies, with a second peak in the alpha band (at 9–11 Hz). The topographies of phase-RT relationships in the theta and alpha bands were highly consistent (Fig. 2 and 3), suggesting that these effects reflect the same neural generators. The presence of phase-RT relationships across multiple frequencies is consistent with previous findings[56, 63, 76, 77]. We have

previously linked different behaviorally relevant frequencies, for example, to different functionally defined cell types (via spike-LFP phase coupling)[56]. Future research (e.g., using intracortical recordings in non-human primates) will need to better parse the functional overlap and/or segregation between theta- and alpha-band activity (i.e., the specific functions associated with behaviorally relevant theta- and alpha-band activity).

Dual-task designs have previously been used to demonstrate interactions between environmental information and internally stored information[30-32, 34, 35, 37, 38]. The present results revealed differences in behavioral performance when to-be-detected information matched to-be-remembered information (Fig. 4B, C), with these 'match effects' decreasing over time (i.e., at longer delays, see also[31]). The present results further demonstrate that match effects only occurred when the external and internal information shared a spatial location. We specifically observed worse discrimination of a visual target (i.e., a noise-added grating) when its orientation and spatial location matched the orientation and spatial location of a to-be-remembered item, suggesting that the neural representation of the to-be-remembered item interfered with perception of the visual target (i.e., on external-probed, dual-task trials). These behavioral findings therefore point to shared neural resources for representing environmental information and internally stored information. Differences in ERPs in response to visual targets that either matched or did not match to-be-remembered items also point to shared neural resources (Fig. 4D, E). Match effects in ERPs occurred shortly after the onset of the visual target (i.e., peaking at 75 ms), during a time period typically associated with the earliest stages of sensory processing[81]. While EEG topographies can be difficult to interpret, the timing of these effects is consistent with previous evidence that neural representations of to-be-remembered items, during working memory, are at least partly encoded in sensory cortices[72, 87-90]. Mirroring our behavioral results, match effects in ERPs were only present on short-delay trials (i.e., trials with a delay less than 1.4 seconds). The absence of match effects on long-delay trials might reflect a transition from the representation of low-level visual features (for to-be-remembered items) to a

more abstract representation. Such a transition would decrease the competition for neural resources between working memory and ongoing perception[31, 75, 91, 92].

Finally, we tested whether the observed behavioral and ERP interactions between environmental and internally stored information (Fig. 4)—specifically, when to-be-detected information matched to-be-remembered information (i.e., match effects)—were modulated by theta phase (i.e., by theta-rhythmic sampling). We therefore compared match effects after sorting short-delay (< 1.4 seconds) trials into two theta-phase bins: a bin centered on the 'good' theta phase (i.e., the pre-probe theta phase associated with better behavioral performance) and a bin centered on the 'bad' theta phase (i.e., the pre-probe theta phase associated with worse behavioral performance). Here, our analyses should be considered exploratory, as our trial counts were low (i.e., the mean was 29.4 trials per subject/condition). While accuracy was generally higher during the 'good' theta phase (relative to the 'bad' theta phase), match effects were present in both theta-phase bins (i.e., there was no interaction between the theta phase and match effects). Although the theta-binned ERPs did not reveal significant clusters, the results are similarly suggestive of early match effects in both theta-phase bins, consistent with the behavioral results. The present behavioral and electrophysiological results therefore indicate that to-be-remembered information interferes with ongoing perception, regardless of pre-probe theta phase. We and others have previously reported evidence that the strength of neural representations for to-be-remembered items—or the amount of information about to-be-remembered items—waxes and wanes as a function of theta phase (and theta-dependent, higher-frequency phase)[63-65, 67]. In the present data, the neural representations of to-be-remembered items that contributed to match effects—which occurred during early sensory processing stages (Fig. 4E)—seemingly did not fluctuate with theta phase (Fig. 5). Combining previous research with the present results, we therefore propose that fluctuations in behavioral performance, associated with theta-rhythmic sampling, do not reflect changes in the neural representations of external and internal information during the earliest sensory processing

stages. Fluctuations in behavioral performance might instead reflect changes to (i) the neural representations in higher-order regions (e.g., prefrontal cortex[64]) and/or (ii) the higher-order cognitive functions that access (or sample) those neural representations[52, 56, 77].

The present findings demonstrate that theta-rhythmic sampling reflects a more general process for selecting and boosting behaviorally relevant information, regardless of whether that information is sampled from the environment or sampled from internal memory stores. That is, there is a theta-rhythmic, domain-general process—with a shared neural basis—for periodically enhancing either external or internal information. While this process seems to be shared between external and internal sampling, there are likely other aspects of external and internal sampling that are domain specific[85, 91, 93, 94]. Future research will need to (i) determine the specific neural circuits through which this sampling process interacts with neural representations of environmental and internally stored information, and (ii) determine the extent to which environmental information and internally stored information can be concurrently sampled.

FIGURES

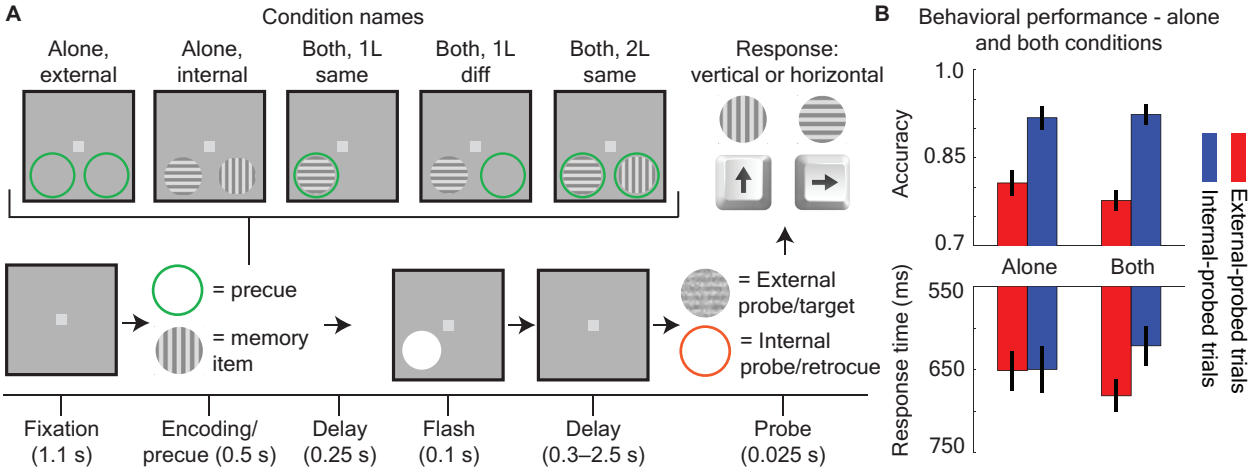

Figure 1. *Experimental task and behavioral data.* (A) Participants reported horizontal or vertical gratings in response to either a noise-added grating (i.e., on external-probed trials) or a retro-cue (i.e., on internal-probed trials). Either pre-cues and/or memory items indicated whether the present trial was an external-only trial, an internal-only trial, or a dual-task trial. (B) Accuracy and response times (n = 25) for 'alone' trials and dual-task trials (i.e., 'both' trials), separately for trials that probed external sampling (red) and trials that probed internal sampling (blue). Error bars indicate standard errors. Supplemental Figure 1 shows the behavioral results separately for the different dual-task conditions.

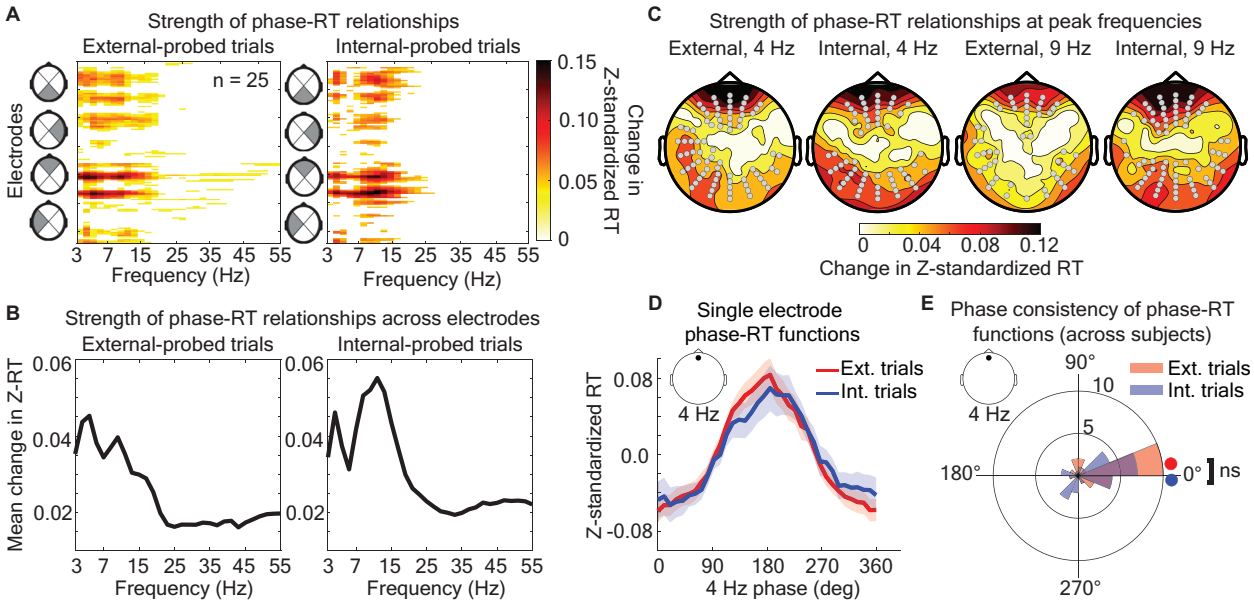

Figure 2. *Phase-RT relationships are consistent across external- and internal-probed trials.* (A) Strength of statistically significant ($p < 0.05$) phase-RT relationships for all electrode (1–128) and frequency combinations (3–55 Hz), separately for external- and internal-probed trials (after combining dual-task conditions). All non-significant combinations have been zeroed. Supplemental Figure 2B shows the same results without zeroing non-significant combinations. (B) Strength of phase-RT relationships after averaging across electrodes, indicating the frequencies that generally have the strongest phase-RT relationships. (C) Topographies and significant electrodes for phase-RT relationships at 4 Hz and 9 Hz. (D) Phase-RT functions for external- versus internal-probed trials (at 4 Hz) for a single, frontal electrode (i.e., the electrode with the strongest phase-RT relationship). (E) The circular distribution, across subjects (n = 25), of phases (at 4 Hz) associated with faster RTs (i.e., the 'good' phase). The red and blue dots indicate the mean 'good' phase across participants for external- and internal-probed trials, respectively.

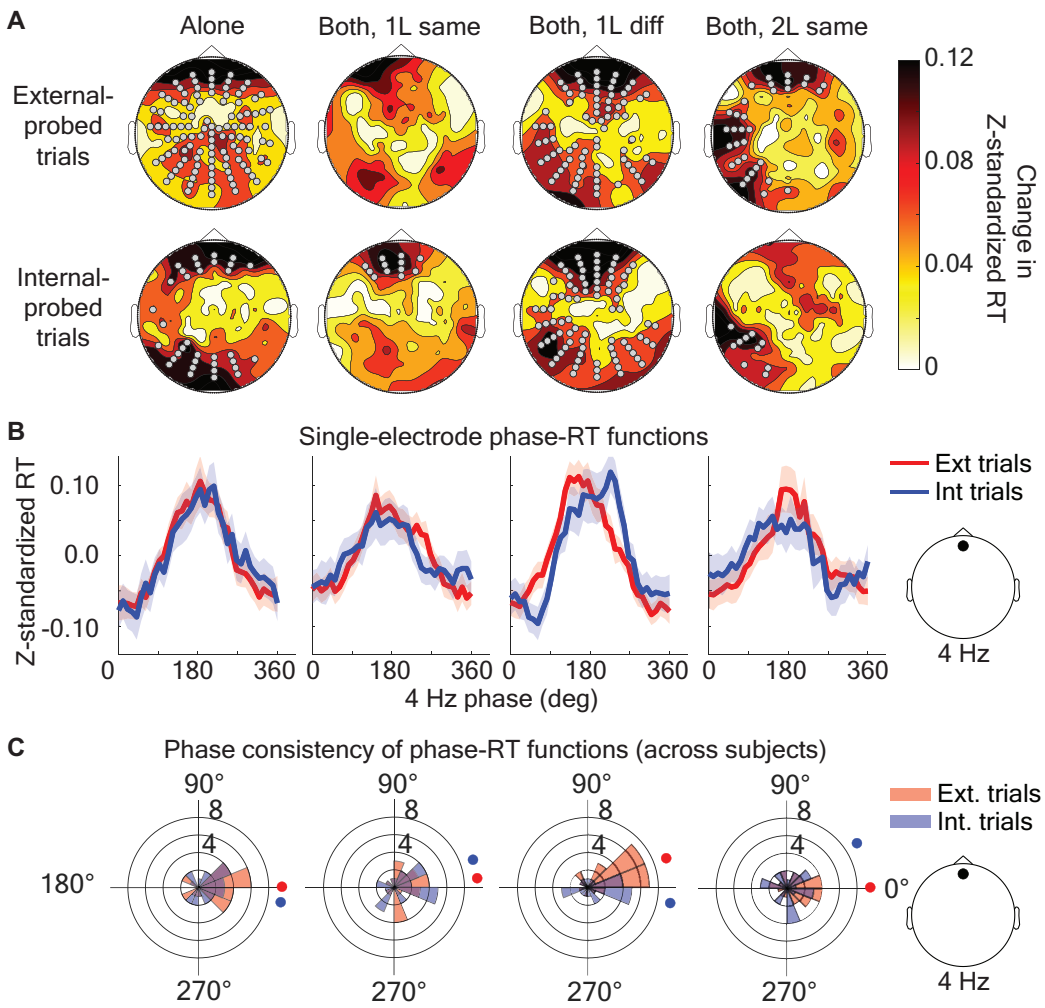

Figure 3. *Phase-RT relationships are consistent across conditions.* (A) Topographies and significant electrodes for phase-RT relationships across the different alone and dual-task conditions, separately for external- and internal-probed trials. (B) Phase-RT functions for external- and internal-probed trials for a single, frontal electrode (i.e., the electrode with the strongest phase-RT relationship). (C) The circular distribution, across subjects (n = 25), of phases associated with faster RTs (i.e., the 'good' phase), separately for the different alone and dual-task conditions. The red and blue dots indicate the mean 'good' phase across participants for external- and internal-probed trials, respectively. All the displayed results are associated with phase measurements at 4 Hz. Supplemental Figure 3 shows the same results but with phase measurements at 9 Hz.

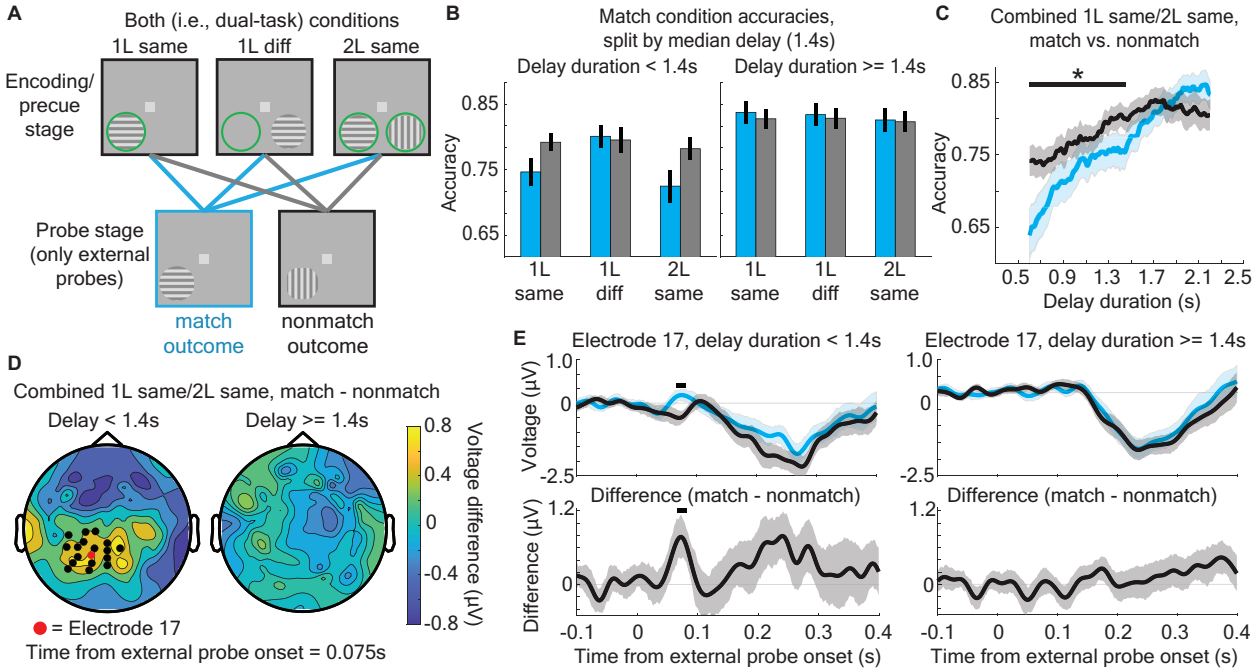

Figure 4. *Internally stored information interferes with environmental information, specifically during trials with shorter delays.* (A) Illustration of 'match' (i.e., the external probe matches the internal representation) and 'non-match' (i.e., the external probe does not match the internal representation) outcomes for dual-task trials that probed external sampling. External probes in the actual task were noise-added gratings (see Fig. 1), but here are depicted as noiseless gratings. (B) Accuracies for external-probed trials that either matched (blue) or did not match (gray) internal representations, for short and long delays (i.e., split by median delay length) and the different dual-task conditions. (C) Accuracies over time for dual-task conditions where the match or non-match occurred at the same spatial location (i.e., the 'both, 1L same' and the 'both, 2L same' conditions). Here, median RTs are calculated over 0.6-second widows, shifted by 0.01 second increments. (D) Topographies of the difference between probe-locked ERPs for match and non-match trials (combined across the 'both, 1L same' and the 'both, 2L same' conditions) at 0.075 seconds (i.e., 75 ms) after the probe occurred, separately for short- and long-delay trials. (E) Probe-locked ERPs and the difference waves for match and non-match trials, specifically for the electrode at the center of the significant cluster (see Fig 4D). Again,

results are shown separately for short- and long-delay trials. All error bars represent standard errors.

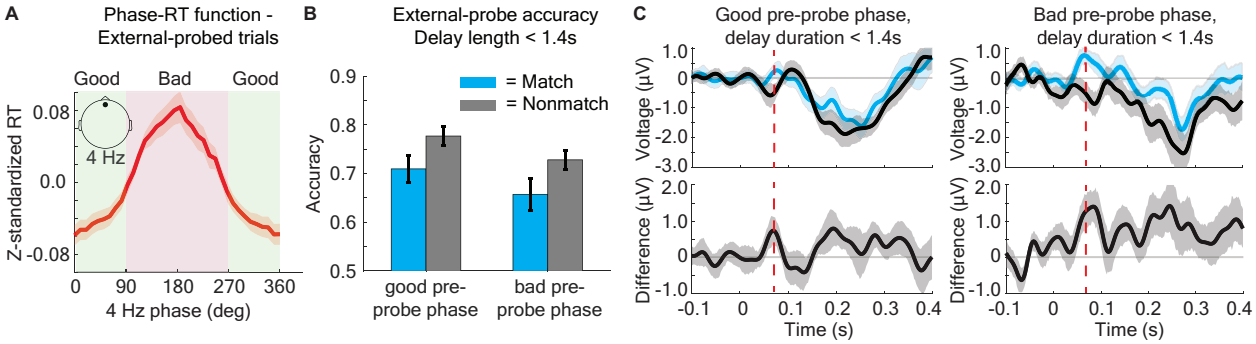

Figure 5. *Match effects during short-delay trials are not dependent on theta phase.* Match effects on short-delay trials (see Fig. 4) were re-examined after (A) first binning by the theta phases (at 4 Hz) associated with either better or worse behavioral performance. (B) Accuracies for match and non-match trials, separately for the 'good' and 'bad' theta-phase bins. (C) Probe-locked ERPs and the difference waves for match and non-match trials, separately for the 'good' and 'bad' theta-phase bins. All error bars represent standard errors.

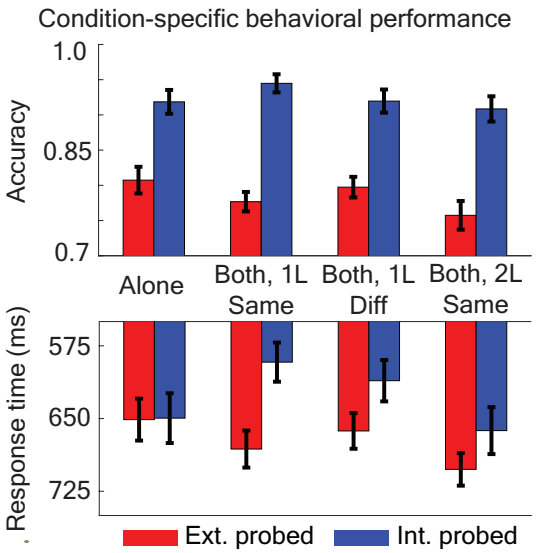

Supplemental Figure 1. *Behavioral results for the alone and dual-task conditions.* Accuracy and response times (n = 25) for the alone and dual-task conditions, separately for trials that probed external sampling (red) and trials that probed internal sampling (blue). Error bars indicate standard errors.

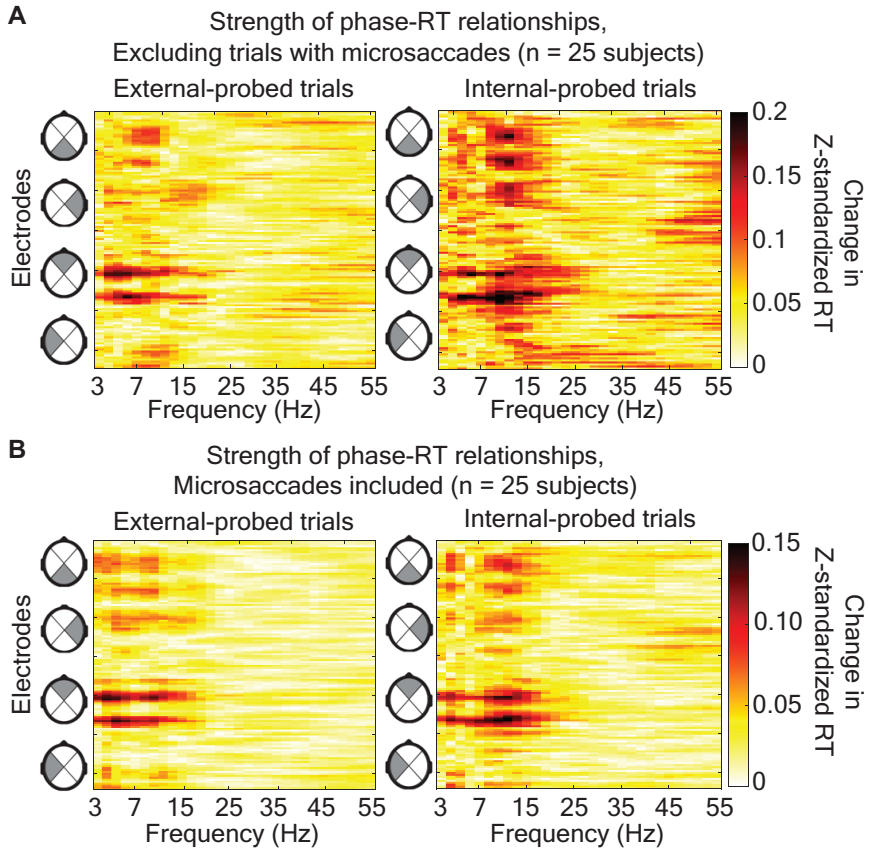

Supplemental Figure 2. *Phase-RT relationships are consistent after excluding trials with microsaccades.* (A) Phase-RT relationships for all electrode (1–128) and frequency (3–55 Hz) combinations, separately for external- and internal-probed trials (combining dual-task conditions), after excluding trials with microsaccades. (B) Phase-RT relationships for all electrode and frequency combinations, separately for external- and internal-probed trials (combining dual-task conditions), including trials with microsaccades.

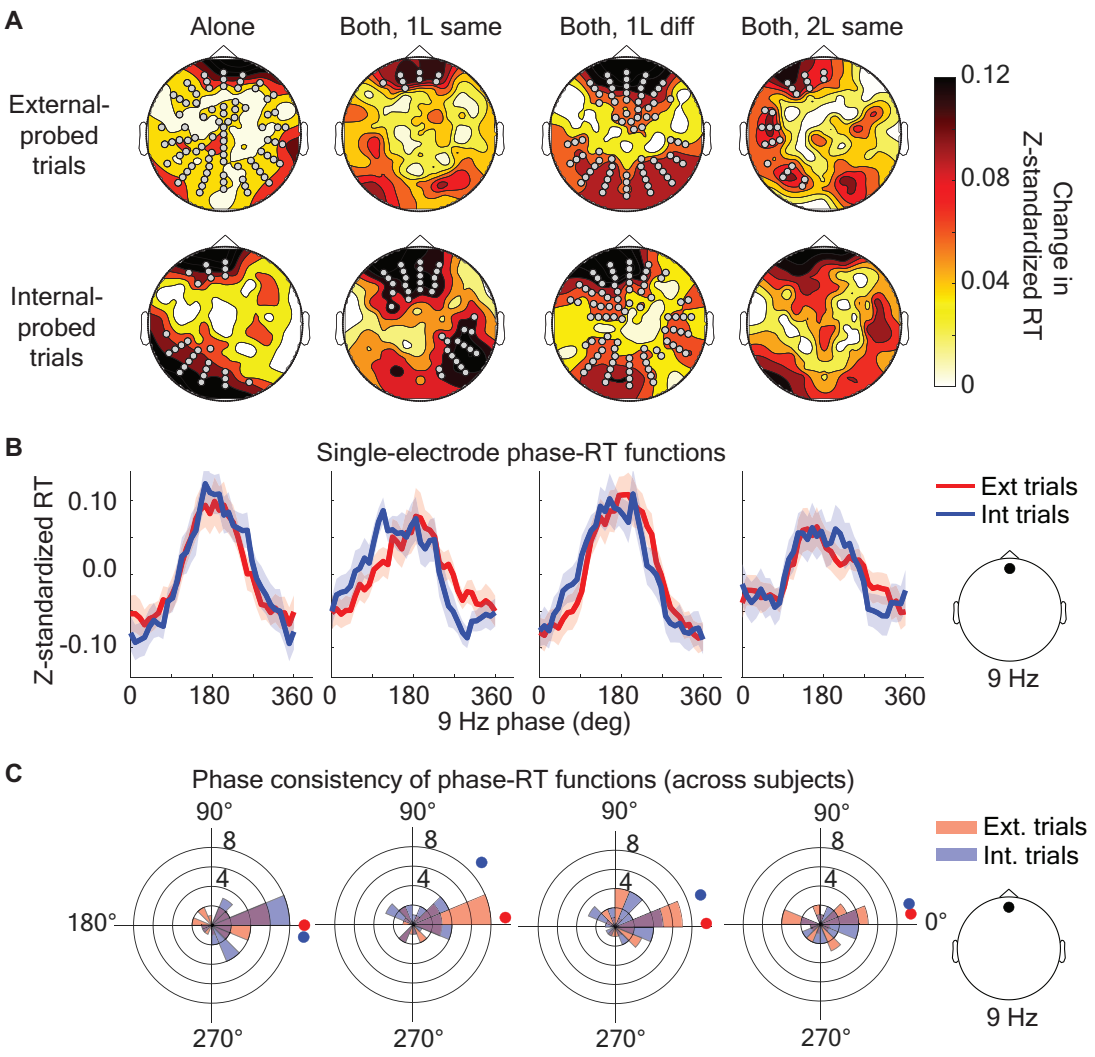

Supplemental Figure 3. *Phase-RT relationships (at 9 Hz) are consistent across trial subtypes.* (A) Topographies and significant electrodes for phase-RT relationships across the different alone and dual-task conditions, separately for external- and internal-probed trials. (B) Phase-RT functions for external- and internal-probed trials for a single, frontal electrode (i.e., the electrode with the strongest phase-RT relationship). (C) The circular distribution, across subjects, of phases associated with faster RTs (i.e., the 'good' phase), separately for the different alone and dual-task conditions. The red and blue dots indicate the mean 'good' phase across participants for external- and internal-probed trials, respectively. All the displayed results are associated with phase measurements at 9 Hz. Figure 3 shows the same results but with phase measurements at 4 Hz.

ACKNOWLEDGEMENTS

This work was supported by grants from the National Science Foundation (NSF 2120539) and the Searle Scholars Program to I.C.F, and from the National Institutes of Health (NEI T32EY007125) to P.C. We would like to thank Miral Abdalaziz and Jordan Klembczyk for their help with data collection.

MATERIALS AND METHODS

Participants

Thirty-one individuals (18 females), aged 19-33 years old (average 23.5), participated in the experiment. Participants completed two sessions of approximately two hours each, separated by at least 24 hours and no more than two weeks. For their time, the participants received $15 per hour. All participants had normal or corrected-to-normal vision and no history of neurological conditions. In accordance with the Declaration of Helsinki, each participant gave written informed consent prior to data collection. The study protocol was approved by the University of Rochester Research Participants Review Board. We excluded six participants from the analyses because of excessive noise in their EEG signals, resulting in the rejection of greater than 20 percent of trials (see below for a description of preprocessing).

Behavioral task

The behavioral task is illustrated in Figure 1A. Participants were seated in a quiet and light-attenuated recording booth in front of a 24-inch LCD monitor (ASUS Predator, 100 Hz refresh rate). Head position and viewing distance were controlled with a fixed chin rest, positioned 57 cm from the screen. At the start of each session, the experimenter explained the behavioral task to the participant, who was then given practice trials until they demonstrated an understanding of the task. The participants used a keyboard to initiate trials (i.e., trials were self-paced) and to give responses. Throughout all trial stages, until a response was given,

participants were required to maintain fixation on a small gray square (0.5 x 0.5 degrees) at the center of the screen. We measured eye position with an EyeLink 1000 Plus (SR Research, Ontario, Canada), which samples both eyes at 2000 Hz. If the position of a participant's eyes deviated by more than one degree from central fixation, the trial was aborted and a new trial was initiated. Aborted trials did not increment the trial count for each block (i.e., each participant completed the same number of trials).

We used Presentation software (Neurobehavioral Systems, Albany, CA, USA) to control the presentation of stimuli and to log responses. Trials consisted of seven sequential stages (see Fig. 1A): a 1100 ms fixation/baseline period, a 500 ms cueing/encoding period, a 250 ms delay, a 100 ms flash event, a variable delay of 300–2500 ms (sampled uniformly), a 25 ms probe, and a response period (with a response cutoff at 2000 ms). All task stimuli were presented at either of two locations: one location to the right of central fixation and one location to the left of central fixation. Both locations were below the horizontal meridian, at a distance of 8 degrees from fixation. Gratings (i.e., memory items and external probes) were 4 degrees in diameter and cues (i.e., pre-cue and retro-cue) were 4.4 degrees in diameter. During the encoding/pre-cueing period, combinations of two types of stimuli could be presented: green circles (i.e., pre-cues to sample external information) and/or square-wave gratings (i.e., to-be-remembered items). Green circles during the encoding/pre-cueing period indicated the potential location(s) for an upcoming, noise-added grating (i.e., an external probe). Cue validity of each green circle depended on the number of other stimuli in the cue array; for example, the green circle in the "both, 1L same" condition was 50% valid (2 total stimuli—one green circle, one grating). Noiseless gratings presented during the encoding/pre-cueing period were memory items to be maintained in anticipation of a potentially upcoming orange circle, which served as a retro-cue[1] (i.e., an internal probe). The encoding period was followed by a brief, 250 ms delay and then a task-irrelevant, 100 ms flash event (i.e., a white circle). This flash event occurred at a previous stimulus location, with equal probability when there were two stimulus locations. Flash

events, which have been similarly utilized by previous studies, create consistent sampling patterns across trials when there are multiple target locations[54, 57, 63]. After the flash event there was a variable delay, 300–2500 ms, when participants needed to (i) maintain memory representations of to-be-remembered gratings (i.e., until a retro-cue), (ii) boost sensory processing in anticipation of an upcoming, noise-added grating (i.e., a target), or (iii) both. Finally, either a target—a noise-added, vertical or horizontal grating—presented with equal probability—or a retro-cue[47] (i.e., an orange circle) occurred. The response scheme was the same for both externally probed trials (i.e., target trials) and internally probed trials (i.e., retro-cue trials): participants made a two-alternative choice, pressing the 'right arrow' on the keyboard to indicate a horizontal grating and the 'up arrow' on the keyboard to indicate a vertical grating. On dual-task trials, which required both external and internal sampling (i.e., 'both' trials), the probe type was determined randomly, with equal probability. That is, while participants anticipated the possibility of either an external probe or an internal probe on dual-task trials, only one or the other was presented following the variable delay. On trials where only external or internal information was presented during the encoding/pre-cueing period (i.e., 'alone, external' and 'alone, internal' trials), the probe type was always the same as the information (e.g., memory items on an 'alone, internal' trial were always followed by a retro-cue). The behavioral task included the following trial types (see Fig. 1A): external sampling only (i.e., 'alone, external'), internal sampling only (i.e., 'alone, internal'), both external and internal sampling at one location (i.e., 'both, 1L same), both external and internal sampling at different locations (i.e., 'both, 1L different'), and both external and internal sampling at both locations ('both, 2L same').

The deployment of attentional resources during external sampling was promoted by using a noise-added grating as the external probe (i.e., target). To generate noise-added gratings, a matrix of uniformly distributed random values was added to square-wave gratings. Importantly, this matrix was multiplied by a scalar 'difficulty constant,' with a value of zero meaning no noise. This scalar determined the contrast of the dark/light stripes and served as

the difficulty parameter for our staircasing procedure. The noise-added gratings (or noiseless gratings, in the case of to-be-remembered items) were min-max normalized to grayscale RGB values between 140 and 220. Every grating stimulus presented during the experiment therefore had the same mean grayscale RGB value as the background (i.e., 180), and the same minimum (i.e., 140) and maximum (i.e., 220) values. This ensured that the brightness of the gratings was always the same, differing only in the coherence of the vertical or horizontal stripes. Figure 1A shows an example of a noise-added grating (i.e., an external probe/target). The amount of noise added to the external probe was calibrated for each participant to achieve 80% accuracy across 'alone, external' trials. Here, we used a staircasing algorithm: on every trial, the accuracy (i.e., the proportion of correct trials) of all previous trials in the 'alone, external' condition (throughout the session) was calculated. If the accuracy was lower than 0.78, the 'difficulty constant' (see above) was lowered. If the accuracy was higher than 0.82, the 'difficulty constant' was increased. To maximize the effectiveness of this procedure, we started each experiment with a 'baseline' block of 50 'alone, external' trials (and no other trial types). Data from this baseline block were excluded from all analyses.

Behavioral analyses

We first compared accuracy and response times (RTs) across the 'alone' conditions (i.e., 'alone, external' and 'alone, internal') and the combined dual-task conditions (i.e., all the 'both' conditions). For all analyses, we split dual-task trials depending on whether external or internal sampling was probed (see Fig. 1B). To test for significant behavioral differences, we conducted repeated measures ANOVAs with follow-up t-tests. The significance threshold for all statistical testing was $p < 0.05$. In addition to testing for behavioral differences between 'alone' and 'both' trials (i.e., the effects of multi-tasking on behavioral performance), we further compared behavioral performance for (i) 'both' trials when the external probe (i.e., a noise-added grating) was a 'match' for a previously presented memory item (i.e., a noiseless grating), relative to (ii)

‘both’ trials when the external probe was a ‘nonmatch’ for a previously presented memory item. Depending on the specific condition, matches in orientation could occur at either the same spatial location or at different spatial locations (see Fig. 4A). Given previous evidence that differences in ‘match’ and ‘non-match’ trials (i.e., interactions between external and internal sampling) change over time[31], trials were further binned based on whether the delay period was greater than or less than the median (i.e., 1400 ms). Finally, to more precisely visualize temporal differences in behavioral performance between ‘match’ and ‘non-match’ trials over time (Fig. 4C), we calculated accuracy within 600-ms bins (e.g., for delays between 300–900 ms), with a step size of 10 ms (e.g., 300–900 ms, 310–910 ms, 320–920 ms…). Here, we combined the same-location conditions (i.e., the conditions that showed significant ‘match’ effects in the previous analysis, see Fig. 4B). For these windowed accuracy comparisons, we conducted a cluster-based approach[78] to control for multiple comparisons between windows (see “cluster-based statistics in phase-behavior and windowed match vs. nonmatch analyses” section).

Data acquisition and preprocessing

We recorded electroencephalographic (EEG) signals at a rate of 2048 Hz, using a 128-channel ActiveTwo BioSemi system (Amsterdam, the Netherlands). For all preprocessing and data analyses, we used a combination of customized MATLAB functions (MathWorks, Natick, MA, USA) and the Fieldtrip toolbox (Donders Institute for Brain, Cognition, and Behavior, Radboud University Nijmegen, the Netherlands)[95]. We downsampled the EEG data to 512 Hz and re-referenced using the 128-electrode average (i.e., an average reference). We then used a discrete Fourier Transform (DFT) filter—applied at 60, 120, and 180 Hz—to remove line noise. After epoching trials from 4.5 seconds before the probe to 1.0 second after the probe, we linearly detrended and demeaned the trial-level data. Trials with either eye blinks or saccades (> 1 degree) were aborted during recording sessions, so there was no need for rejection/correction

based on eye artifacts during the initial preprocessing. We used voltage threshold of ±100 μV for identifying trials/channels with other noise transients, interpolating electrodes that exceeded this threshold using the nearest neighbor spline[96]. If more than 10% of electrodes needed to be interpolated on a single trial, we excluded the trial from further analyses[7]. If more than 20% of trials were excluded for a given participant, we excluded all of the participant's data from further analyses (n = 6). The remaining participants (n = 25) had an average of 6% of trials removed during artifact rejection, leaving an average of 939 trials per participant (across all conditions).

Match vs. nonmatch statistics and probe-locked event related potentials (ERP)

In addition to comparing behavioral performance for dual-task trials—when an external probe (i.e., a noise-added grating) matched a to-be-remembered item versus when an external probe did not match a to-be-remembered item (Fig. 4B, C)—we also compared condition-specific event-related potentials (ERPs). Based on the results of the behavioral analysis (Fig. 4B), which revealed 'match effects' only when the external probe matched both the orientation and the spatial location of a to-be-remembered item (i.e., a noiseless grating), we calculated ERPs for 'match' and 'non-match' trials after combining the 'both, 1L same' and the 'both, 2L same' conditions (i.e., the conditions when external probes could be presented at the same location as a previously presented to-be-remembered item, see Fig. 1A). To calculate the probe-locked ERPs, we first averaged the pre-processed data across trials, for each participant, from 0.1 seconds before probe onset to 0.4 seconds after probe onset. For display purposes, we then grand-averaged the ERPs across participants and applied a 30 Hz lowpass filter (Fig. 4E). To test whether ERPs for 'match' trials significantly differed from ERPs for 'non-match' trials, we used a cluster-based approach to correct for multiple comparisons, across electrodes and timepoints[78] (see "cluster-based statistics in phase-behavior and windowed match vs. nonmatch analyses" section). Based on the results of the present behavioral analyses (Fig. 4B, C) and

prior research[31], we conducted this analysis separately for trials that were greater than or less than the median delay length (i.e., 1.4 seconds).

Measuring phase-behavior relationships

We calculated phase-behavior relationships to determine if RTs and/or accuracy varied as a function of frequency-specific phase, measured just prior to probe onset (i.e., during the variable delay, just prior to the presentation of either a visual target or a retro-cue)[76]. Here, we first used Morlet wavelet convolution to derive frequency-specific phase measurements for each trial (from 3–55 Hz). To avoid contamination of the phase estimates from either flash-evoked visual responses or probe-evoked visual responses, (i) trials with delay periods less than 650 ms were excluded from the analyses (i.e., to avoid probe-evoked visual responses) and (ii) the time point for each phase measurement (i.e., the center of the wavelet) was half a wavelet width (i.e., half the temporal extent of the wavelet) from probe onset. That is, the wavelet was fit for each frequency such that the last time point included for calculation of the phase measurement was the time point just prior to probe onset. For example, phase for the 4 Hz, 2-cycle wavelet—with a temporal extent of 500 ms—was measured 250 ms prior to probe onset (i.e., the wavelet was centered 250 ms prior to probe onset). We calculated phase estimates from 3–8 Hz, in 1-Hz increments, and from 9–55 Hz, in 2-Hz increments. The number of cycles per wavelet was 2 for wavelets from 3–8 Hz and increased logarithmically from 2 to 5 cycles for wavelets from 9–55 Hz.

After obtaining electrode- and frequency-specific phase measurements (from 3–55 Hz), we paired trial-specific phase measurements with trial-level RTs. Normalization of RTs was done within participant and condition of interest. We then binned z-RTs by electrode- and frequency-specific phase, using bins with a width of 180 degrees (e.g., 0 to 180 degrees), shifted in 10-degree steps (e.g., 0 to 180 degrees, 10 to 190, etc.). Following this binning procedure, we calculated the median RT for each bin, providing z-RT as a function of

frequency-specific phase for each electrode and condition of interest. We next averaged the participant-level phase-RT functions (n = 25) to determine the frequencies and electrodes with the strongest phase-RT relationships. We calculated phase-accuracy functions using a nearly identical procedure, except that the proportion of correct trials was calculated for each phase bin, rather than median z-RT. Because accuracy was at ceiling for internally probed trials (i.e., retro-cued trials), we only calculated phase-accuracy functions for externally probed trials (i.e., target trials). Similar to previous studies[56] we hypothesized that the phasic modulation of behavioral performance would have a “peak” and a “trough” (i.e., a “good” phase and a “bad” phase) that were separated by approximately 180 degrees. The strength of the grand-averaged phase-behavior functions was therefore summarized by the amplitude of a one-cycle sine wave. We specifically used a discrete Fourier transform (DFT) applied to each grand-averaged function (at each frequency and electrode), with the absolute value of the second component of the DFT output being used to approximate the amplitude of a one-cycle sine fit to the phase-behavior function[76].

To determine the statistical significance of phase-behavior relationships, we randomly shuffled the observed phases and RTs (1500 permutations) before recalculating the strength of the phase-behavior relationships (following the same procedure outlined above). We then compared the observed values to the null distribution of randomized values, separately for each condition, to calculate p-values (i.e., the proportion of values in the null distribution that exceeded the observed value) for all electrodes and frequencies. Finally, we applied cluster-correction to correct for multiple comparisons, which has been widely used for EEG and MEG analyses[78] (see “cluster-based statistics in phase-behavior and windowed match vs. nonmatch analyses” section).

To determine whether the ‘good’ phases (i.e., the phases associated with better behavioral performance) differed between external and internal sampling, we compared the distributions of ‘good’ phases across participants for the conditions of interest (i.e., external

sampling vs. internal sampling). Here, the analyses were limited to the frequencies and electrodes where the strongest phase-behavior relationships were observed during previous analyses. We used a circular Watson-Williams test to determine whether the participant-level distribution of 'good' phases during external sampling significantly differed from the participant-level distribution of 'good' phases during internal sampling (Fig. 2E)[63].

Excluding trials with microsaccades from phase-behavior relationships

Like behavioral performance, previous research has demonstrated that the likelihood of microsaccades (i.e., fixational eye movements) is modulated as a function of theta phase[79]. Previous work has also shown that phase-behavior relationships persist after excluding trials with microsaccades, indicating that phase-behavior relationships are not attributable to microsaccades[56]. We conducted a control analysis with the present data to similarly confirm that phase-behavior relationships are not attributable to microsaccades. That is, we re-calculated phase-behavior relationships after excluding trials with microsaccades during the delay period (i.e., in the pre-probe period).

To distinguish microsaccadic events, we set the EyeLink online parser parameters to a velocity threshold of 22 degrees/sec, acceleration threshold of 4000 degrees/sec^2, and travel distance of <1 visual degree. Using these criteria, on average, each participant had 522 trials with at least one microsaccade. To test whether the relationship between theta phase and behavioral performance was attributable to these small, fixational eye movements (i.e., microsaccades), we re-calculated phase-behavior relationships (see previous section) after excluding these trials (Supplementary Fig. 2A). After excluding trials with microsaccades, there were an average of 376 trials remaining per subject. It is important to note that the measured strength of phase-behavior relationships depends on trial counts (as do other phase-based coherence measures, such as inter-trial phase coherence). Therefore, the scale of results with and without microsaccades (in Supplementary Figure 2) is not comparable (i.e., due to lower

trial counts in the analyses without microsaccades). This control analysis revealed that the pattern of phase-behavior results is qualitatively similar, regardless of whether trials with microsaccades are included or excluded from the analyses.

“Good” vs. “bad” theta bin analyses

To measure the potential effect of rhythmic dynamics on the interaction between external and internal sampling, we performed match effect analyses separately for “good” and “bad” theta bins (i.e., theta-phase bins associated with either better or worse behavioral performance). To define these bins, we used the phase-RT function for external sampling at the center of the frontal cluster, at 4 Hz, and separated the peak and trough of performance (Fig. 5A). Good-phase trials were defined as trials with pre-probe phases less than 90° and greater than 270°, while bad-phase trials were defined as trials with pre-probe phases greater than 90° and less than 270°. For each of these theta bins, we calculated accuracy for the combined ‘both, 1L same’ and ‘both, 2L same’ conditions with short delays (<1.4s), separately for ‘match’ and ‘nonmatch’ trials. We similarly recalculated the probe-locked ERPs after binning trials based on theta phase (for more details see “Match vs. nonmatch statistics and probe-locked ERPs”). After binning ‘match’ and ‘nonmatch’ trials by theta phase, there was a mean of 29.4 trials per subject/condition.

Cluster-based statistics in phase-behavior and windowed match vs. nonmatch analyses

We statistically accounted for multiple comparisons and the autocorrelation of behavioral and EEG time-series data over spatial, temporal, and spectral dimensions by applying a nonparametric “cluster-correction” method, which has been widely used in electrophysiological research[4]. Procedurally, this method involves four main steps. First, a distribution of 1500 “null observations” was generated by repeatedly randomizing the data and recalculating the results (see below paragraph for details on how this was specifically done for phase-behavior and

windowed match vs. nonmatch analyses). Second, a distribution of "null cluster magnitudes" was created from this distribution of "null observations". To calculate the magnitude of one null cluster, we first calculated the p-value of each null observation, relative to the rest of the null observations (i.e., the null distribution). Then, the p-values that crossed the significance threshold ($p<0.05$) were put into "clusters." The clusters were defined by consecutively adjacent significant values. Adjacency is defined in the spatial domain as electrodes that are directly next to each other on the scalp, in the frequency domain as frequencies that are directly previous or next in sequence (e.g. 4 Hz is adjacent to 5 Hz), and in the temporal domain as timepoints that are directly before or after (e.g. for a 100 Hz sampling rate time series, 0.01s is adjacent to 0.02s, which is adjacent to 0.03s, etc…). Therefore, a cluster represents a grouping of significant values that are unbroken in adjacency across N dimensions. We calculated the magnitude of a cluster by summing 1/p-value of each point in the cluster. This means that a high-value cluster will contain values that have a strong effect (e.g., higher phase-behavior strength or a greater difference in accuracy or voltage) and cover many points in the N-dimensional range of points, while a low-value cluster does not have many significant values and these values have a low effect. After calculating the null clusters for one null observation, the magnitude of the largest null cluster was recorded. For 1500 permutations from the first step, this means 1500 null cluster magnitudes assuming the null hypothesis. Third, the real cluster magnitudes were calculated. This follows the same procedure as step two above, except the real observations are clustered against the null distribution of observations. Once again, this results in a grouping of $p<0.05$ significant values that have unbroken adjacence. Fourth, the real cluster magnitudes are compared against the null distribution of cluster magnitudes. This resulted in each observed cluster receiving its own p-value compared to the distribution of null-clusters. For cluster-corrected analyses, only the observed values within clusters of $p<0.05$ magnitude was treated as significant. In summary, a significant value within a significant cluster indicates that not only was this value $p<0.05$ significant compared to random permutations, but

that the magnitude and number of consecutively adjacent values was also significant compared to the null hypothesis.

In the first step described above, a null distribution of observations is needed to create the null clusters which will be compared against the observed clusters. This was done differently for the phase-behavior and match vs. nonmatch analyses. For phase-RT relationships (Figs. 2 and 3), the null hypothesis is that there is no relationship between phase and response times. The null distribution is therefore generated by randomizing trial-level phase measurements relative to trial-level RTs (i.e., by breaking the potential relationship between phase and RTs). For 'match' vs. 'non-match' analyses (Figs. 4 and 5), the null distribution was generated by randomizing trials across the 'match' and 'non-match' conditions.

REFERENCES

1. Carrasco M. Visual attention: The past 25 years. Vision research. 2011;51(13):1484-525. doi: 10.1016/j.visres.2011.04.012; PMCID: PMC3390154.
2. Moore T, Zirnsak M. Neural Mechanisms of Selective Visual Attention. Annual review of psychology. 2017;68:47-72. doi: 10.1146/annurev-psych-122414-033400. PubMed PMID: 28051934.
3. Posner MI. Orienting of attention. The Quarterly journal of experimental psychology. 1980;32(1):3-25. Epub 1980/02/01. PubMed PMID: 7367577.
4. D'Esposito M, Postle BR. The cognitive neuroscience of working memory. Annual review of psychology. 2015;66:115-42. Epub 20140919. doi: 10.1146/annurev-psych-010814-015031. PubMed PMID: 25251486; PMCID: PMC4374359.
5. Baddeley A. Working memory. Science. 1992;255(5044):556-9. doi: 10.1126/science.1736359. PubMed PMID: 1736359.
6. Squire RF, Noudoost B, Schafer RJ, Moore T. Prefrontal contributions to visual selective attention. Annual review of neuroscience. 2013;36:451-66. doi: 10.1146/annurev-neuro-062111-150439. PubMed PMID: 23841841.
7. Zanto TP, Rubens MT, Thangavel A, Gazzaley A. Causal role of the prefrontal cortex in top-down modulation of visual processing and working memory. Nature neuroscience. 2011;14(5):656-61. Epub 20110327. doi: 10.1038/nn.2773. PubMed PMID: 21441920; PMCID: PMC3083493.
8. Bisley JW, Mirpour K, Arcizet F, Ong WS. The Role of the Lateral Intraparietal Area in Orienting Attention and its Implications for Visual Search. The European journal of neuroscience. 2011;33(11):1982–90. doi: doi: 10.1111/j.1460-9568.2011.07700.x; PMCID: PMC3164992.
9. Koenigs M, Barbey AK, Postle BR, Grafman J. Superior parietal cortex is critical for the manipulation of information in working memory. The Journal of neuroscience : the official journal of the Society for Neuroscience. 2009;29(47):14980-6. doi: 10.1523/JNEUROSCI.3706-09.2009. PubMed PMID: 19940193; PMCID: PMC2799248.

10. Todd JJ, Marois R. Capacity limit of visual short-term memory in human posterior parietal cortex. Nature. 2004;428(6984):751-4. doi: 10.1038/nature02466. PubMed PMID: 15085133.
11. Xu Y, Chun MM. Dissociable neural mechanisms supporting visual short-term memory for objects. Nature. 2006;440(7080):91-5. Epub 20051228. doi: 10.1038/nature04262. PubMed PMID: 16382240.
12. Reynolds JH, Chelazzi L. Attentional modulation of visual processing. Annual review of neuroscience. 2004;27:611-47. doi: 10.1146/annurev.neuro.26.041002.131039. PubMed PMID: 15217345.
13. Corbetta M, Shulman GL. Control of goal-directed and stimulus-driven attention in the brain. Nature reviews Neuroscience. 2002;3(3):201-15. Epub 2002/05/08. doi: 10.1038/nrn755. PubMed PMID: 11994752.
14. LaBar KS, Gitelman DR, Parrish TB, Mesulam M. Neuroanatomic overlap of working memory and spatial attention networks: a functional MRI comparison within subjects. NeuroImage. 1999;10(6):695-704. doi: 10.1006/nimg.1999.0503. PubMed PMID: 10600415.
15. Mayer JS, Bittner RA, Nikolic D, Bledowski C, Goebel R, Linden DE. Common neural substrates for visual working memory and attention. NeuroImage. 2007;36(2):441-53. Epub 20070320. doi: 10.1016/j.neuroimage.2007.03.007. PubMed PMID: 17462914.
16. Panichello MF, Buschman TJ. Shared mechanisms underlie the control of working memory and attention. Nature. 2021;592(7855):601-5. Epub 20210331. doi: 10.1038/s41586-021-03390-w. PubMed PMID: 33790467; PMCID: PMC8223505.
17. Pasternak T, Greenlee MW. Working memory in primate sensory systems. Nature reviews Neuroscience. 2005;6(2):97-107. doi: 10.1038/nrn1603. PubMed PMID: 15654324.
18. van Kerkoerle T, Self MW, Roelfsema PR. Layer-specificity in the effects of attention and working memory on activity in primary visual cortex. Nature communications. 2017;8:13804. Epub 20170105. doi: 10.1038/ncomms13804. PubMed PMID: 28054544; PMCID: PMC5227065.
19. Huang J, Wang T, Dai W, Li Y, Yang Y, Zhang Y, Wu Y, Zhou T, Xing D. Neuronal representation of visual working memory content in the primate primary visual cortex. Science advances. 2024;10(24):eadk3953. Epub 20240614. doi: 10.1126/sciadv.adk3953. PubMed PMID: 38875332; PMCID: PMC11177929.
20. Chun MM, Golomb JD, Turk-Browne NB. A taxonomy of external and internal attention. Annual review of psychology. 2011;62:73-101. doi: 10.1146/annurev.psych.093008.100427. PubMed PMID: 19575619.
21. Gazzaley A, Nobre AC. Top-down modulation: bridging selective attention and working memory. Trends in cognitive sciences. 2012;16(2):129-35. doi: 10.1016/j.tics.2011.11.014. PubMed PMID: 22209601; PMCID: 3510782.
22. Kiyonaga A, Egner T. Working memory as internal attention: toward an integrative account of internal and external selection processes. Psychonomic bulletin & review. 2013;20(2):228-42. doi: 10.3758/s13423-012-0359-y. PubMed PMID: 23233157; PMCID: 3594067.
23. Awh E, Jonides J. Overlapping mechanisms of attention and spatial working memory. Trends in cognitive sciences. 2001;5(3):119-26. doi: 10.1016/s1364-6613(00)01593-x. PubMed PMID: 11239812.
24. Oberauer K. Working Memory and Attention - A Conceptual Analysis and Review. J Cogn. 2019;2(1):36. Epub 20190808. doi: 10.5334/joc.58. PubMed PMID: 31517246; PMCID: PMC6688548.
25. van Ede F, Nobre AC. Turning Attention Inside Out: How Working Memory Serves Behavior. Annual review of psychology. 2023;74:137-65. Epub 20220812. doi: 10.1146/annurev-psych-021422-041757. PubMed PMID: 35961038.

26. Craik FI, Govoni R, Naveh-Benjamin M, Anderson ND. The effects of divided attention on encoding and retrieval processes in human memory. Journal of experimental psychology General. 1996;125(2):159-80. doi: 10.1037//0096-3445.125.2.159. PubMed PMID: 8683192.
27. Chun MM, Turk-Browne NB. Interactions between attention and memory. Current opinion in neurobiology. 2007;17(2):177-84. Epub 20070326. doi: 10.1016/j.conb.2007.03.005. PubMed PMID: 17379501.
28. Soto D, Hodsoll J, Rotshtein P, Humphreys GW. Automatic guidance of attention from working memory. Trends in cognitive sciences. 2008;12(9):342-8. Epub 20080805. doi: 10.1016/j.tics.2008.05.007. PubMed PMID: 18693131.
29. Lavie N, De Fockert J. The role of working memory in attentional capture. Psychonomic bulletin & review. 2005;12(4):669-74. doi: 10.3758/bf03196756. PubMed PMID: 16447380.
30. Nobre AC, Coull JT, Maquet P, Frith CD, Vandenberghe R, Mesulam MM. Orienting attention to locations in perceptual versus mental representations. Journal of cognitive neuroscience. 2004;16(3):363-73. doi: 10.1162/089892904322926700. PubMed PMID: 15072672.
31. Teng C, Kaplan SM, Shomstein S, Kravitz DJ. Assessing the interaction between working memory and perception through time. Attention, perception & psychophysics. 2023;85(7):2196-209. Epub 20230922. doi: 10.3758/s13414-023-02785-3. PubMed PMID: 37740152.
32. Teng C, Kravitz DJ. Visual working memory directly alters perception. Nature human behaviour. 2019;3(8):827-36. Epub 20190708. doi: 10.1038/s41562-019-0640-4. PubMed PMID: 31285620.
33. Olivers CN, Meijer F, Theeuwes J. Feature-based memory-driven attentional capture: visual working memory content affects visual attention. Journal of experimental psychology Human perception and performance. 2006;32(5):1243-65. doi: 10.1037/0096-1523.32.5.1243. PubMed PMID: 17002535.
34. Soto D, Heinke D, Humphreys GW, Blanco MJ. Early, involuntary top-down guidance of attention from working memory. Journal of experimental psychology Human perception and performance. 2005;31(2):248-61. doi: 10.1037/0096-1523.31.2.248. PubMed PMID: 15826228.
35. Soto D, Humphreys GW, Heinke D. Working memory can guide pop-out search. Vision research. 2006;46(6-7):1010-8. Epub 20051027. doi: 10.1016/j.visres.2005.09.008. PubMed PMID: 16257030.
36. Rademaker RL, Bloem IM, De Weerd P, Sack AT. The impact of interference on short-term memory for visual orientation. Journal of experimental psychology Human perception and performance. 2015;41(6):1650-65. Epub 20150810. doi: 10.1037/xhp0000110. PubMed PMID: 26371383.
37. Swallow KM, Broitman AW, Riley E, Turker HB. Grounding the Attentional Boost Effect in Events and the Efficient Brain. Frontiers in psychology. 2022;13:892416. Epub 20220722. doi: 10.3389/fpsyg.2022.892416. PubMed PMID: 35936250; PMCID: PMC9355572.
38. Swallow KM, Jiang YV. Attentional load and attentional boost: a review of data and theory. Frontiers in psychology. 2013;4:274. Epub 20130520. doi: 10.3389/fpsyg.2013.00274. PubMed PMID: 23730294; PMCID: PMC3657623.
39. Beck VM, Hollingworth A, Luck SJ. Simultaneous control of attention by multiple working memory representations. Psychological science. 2012;23(8):887-98. Epub 20120703. doi: 10.1177/0956797612439068. PubMed PMID: 22760886; PMCID: PMC3419335.
40. Van der Stigchel S, Merten H, Meeter M, Theeuwes J. The effects of a task-irrelevant visual event on spatial working memory. Psychonomic bulletin & review. 2007;14(6):1066-71. doi: 10.3758/bf03193092. PubMed PMID: 18229476.
41. Huang J, Sekuler R. Distortions in recall from visual memory: two classes of attractors at work. Journal of vision. 2010;10(2):24 1-7. Epub 20100224. doi: 10.1167/10.2.24. PubMed PMID: 20462325; PMCID: PMC4104522.

42. Downing PE. Interactions between visual working memory and selective attention. Psychological science. 2000;11(6):467-73. doi: 10.1111/1467-9280.00290. PubMed PMID: 11202491.
43. Konstantinou N, Lavie N. Dissociable roles of different types of working memory load in visual detection. Journal of experimental psychology Human perception and performance. 2013;39(4):919-24. Epub 20130527. doi: 10.1037/a0033037. PubMed PMID: 23713796; PMCID: PMC3725889.
44. Konstantinou N, Bahrami B, Rees G, Lavie N. Visual short-term memory load reduces retinotopic cortex response to contrast. Journal of cognitive neuroscience. 2012;24(11):2199-210. Epub 20120820. doi: 10.1162/jocn_a_00279. PubMed PMID: 22905823.
45. Balestrieri E, Ronconi L, Melcher D. Shared resources between visual attention and visual working memory are allocated through rhythmic sampling. The European journal of neuroscience. 2022;55(11-12):3040-53. Epub 20210512. doi: 10.1111/ejn.15264. PubMed PMID: 33942394.
46. van Ede F, Nobre AC. Toward a neurobiology of internal selective attention. Trends in neurosciences. 2021;44(7):513-5. Epub 20210512. doi: 10.1016/j.tins.2021.04.010. PubMed PMID: 33992457.
47. Souza AS, Oberauer K. In search of the focus of attention in working memory: 13 years of the retro-cue effect. Attention, perception & psychophysics. 2016;78(7):1839-60. doi: 10.3758/s13414-016-1108-5. PubMed PMID: 27098647.
48. Myers NE, Stokes MG, Nobre AC. Prioritizing Information during Working Memory: Beyond Sustained Internal Attention. Trends in cognitive sciences. 2017;21(6):449-61. Epub 20170425. doi: 10.1016/j.tics.2017.03.010. PubMed PMID: 28454719; PMCID: PMC7220802.
49. Murray AM, Nobre AC, Clark IA, Cravo AM, Stokes MG. Attention restores discrete items to visual short-term memory. Psychological science. 2013;24(4):550-6. Epub 20130222. doi: 10.1177/0956797612457782. PubMed PMID: 23436786; PMCID: PMC4138001.
50. Postle BR. Working memory as an emergent property of the mind and brain. Neuroscience. 2006;139(1):23-38. Epub 20051201. doi: 10.1016/j.neuroscience.2005.06.005. PubMed PMID: 16324795; PMCID: PMC1428794.
51. Theeuwes J, Belopolsky A, Olivers CN. Interactions between working memory, attention and eye movements. Acta Psychol (Amst). 2009;132(2):106-14. Epub 20090223. doi: 10.1016/j.actpsy.2009.01.005. PubMed PMID: 19233340.
52. Fiebelkorn IC, Kastner S. A Rhythmic Theory of Attention. Trends in cognitive sciences. 2019;23(2):87-101. doi: 10.1016/j.tics.2018.11.009. PubMed PMID: 30591373.
53. Benedetto A, Morrone MC, Tomassini A. The common rhythm of action and perception. Journal of cognitive neuroscience. 2019;32(2):187-200. doi: 10.1162/jocn_a_01436.
54. Fiebelkorn IC, Saalmann YB, Kastner S. Rhythmic sampling within and between objects despite sustained attention at a cued location. Current biology : CB. 2013;23(24):2553-8. doi: 10.1016/j.cub.2013.10.063. PubMed PMID: 24316204; PMCID: 3870032.
55. Helfrich RF, Fiebelkorn IC, Szczepanski SM, Lin JJ, Parvizi J, Knight RT, Kastner S. Neural mechanisms of sustained attention are rhythmic. Neuron. 2018;99(4):829-41. doi: 10.1016/j.neuron.2018.07.032.
56. Fiebelkorn IC, Pinsk MA, Kastner S. A dynamic interplay within the frontoparietal network underlies rhythmic spatial attention. Neuron. 2018;99(4):842-53. doi: 10.1016/j.neuron.2018.07.038.
57. Landau AN, Fries P. Attention samples stimuli rhythmically. Current biology : CB. 2012;22(11):1000-4. Epub 2012/05/29. doi: 10.1016/j.cub.2012.03.054. PubMed PMID: 22633805.
58. Landau AN, Schreyer HM, van Pelt S, Fries P. Distributed Attention Is Implemented through Theta-Rhythmic Gamma Modulation. Current biology : CB. 2015;25(17):2332-7. doi: 10.1016/j.cub.2015.07.048. PubMed PMID: 26279231.

59. Dugue L, Marque P, VanRullen R. Theta oscillations modulate attentional search performance periodically. Journal of cognitive neuroscience. 2015;27(5):945-58. doi: 10.1162/jocn_a_00755. PubMed PMID: 25390199.
60. Dugue L, Roberts M, Carrasco M. Attention Reorients Periodically. Current biology : CB. 2016;26(12):1595-601. doi: 10.1016/j.cub.2016.04.046. PubMed PMID: 27265395; PMCID: 4935543.
61. VanRullen R, Carlson T, Cavanagh P. The blinking spotlight of attention. Proceedings of the National Academy of Sciences of the United States of America. 2007;104(49):19204-9. doi: 10.1073/pnas.0707316104. PubMed PMID: 18042716; PMCID: 2148268.
62. Busch NA, VanRullen R. Spontaneous EEG oscillations reveal periodic sampling of visual attention. Proceedings of the National Academy of Sciences of the United States of America. 2010;107(37):16048-53. Epub 2010/09/02. doi: 10.1073/pnas.1004801107. PubMed PMID: 20805482; PMCID: 2941320.
63. Abdalaziz M, Redding ZV, Fiebelkorn IC. Rhythmic temporal coordination of neural activity prevents representational conflict during working memory. Current biology : CB. 2023;33(9):1855-63 e3. Epub 20230425. doi: 10.1016/j.cub.2023.03.088. PubMed PMID: 37100058.
64. Siegel M, Warden MR, Miller EK. Phase-dependent neuronal coding of objects in short-term memory. Proceedings of the National Academy of Sciences of the United States of America. 2009;106(50):21341-6. doi: 10.1073/pnas.0908193106. PubMed PMID: 19926847; PMCID: 2779828.
65. Bahramisharif A, Jensen O, Jacobs J, Lisman J. Serial representation of items during working memory maintenance at letter-selective cortical sites. PLoS biology. 2018;16(8):e2003805. Epub 20180815. doi: 10.1371/journal.pbio.2003805. PubMed PMID: 30110320; PMCID: PMC6093599.
66. Peters B, Kaiser J, Rahm B, Bledowski C. Object-based attention prioritizes working memory contents at a theta rhythm. Journal of experimental psychology General. 2021;150(6):1250-6. Epub 20201119. doi: 10.1037/xge0000994. PubMed PMID: 33211526.
67. Kaminski J, Brzezicka A, Mamelak AN, Rutishauser U. Combined Phase-Rate Coding by Persistently Active Neurons as a Mechanism for Maintaining Multiple Items in Working Memory in Humans. Neuron. 2020;106(2):256-64 e3. Epub 20200220. doi: 10.1016/j.neuron.2020.01.032. PubMed PMID: 32084331; PMCID: PMC7217299.
68. Chota S, Leto C, van Zantwijk L, Van der Stigchel S. Attention rhythmically samples multi-feature objects in working memory. Scientific reports. 2022;12(1):14703. Epub 20220829. doi: 10.1038/s41598-022-18819-z. PubMed PMID: 36038570; PMCID: PMC9424255.
69. Pomper U, Ansorge U. Theta-Rhythmic Oscillation of Working Memory Performance. Psychological science. 2021;32(11):1801-10. Epub 20210930. doi: 10.1177/09567976211013045. PubMed PMID: 34592108.
70. Hogendoorn H. Voluntary Saccadic Eye Movements Ride the Attentional Rhythm. Journal of cognitive neuroscience. 2016;28(10):1625-35. doi: 10.1162/jocn_a_00986. PubMed PMID: 27243615.
71. Schroeder CE, Wilson DA, Radman T, Scharfman H, Lakatos P. Dynamics of Active Sensing and perceptual selection. Current opinion in neurobiology. 2010;20(2):172-6. doi: 10.1016/j.conb.2010.02.010. PubMed PMID: 20307966; PMCID: 2963579.
72. Emrich SM, Riggall AC, Larocque JJ, Postle BR. Distributed patterns of activity in sensory cortex reflect the precision of multiple items maintained in visual short-term memory. The Journal of neuroscience : the official journal of the Society for Neuroscience. 2013;33(15):6516-23. doi: 10.1523/JNEUROSCI.5732-12.2013. PubMed PMID: 23575849; PMCID: PMC3664518.

73. Serences JT. Neural mechanisms of information storage in visual short-term memory. Vision research. 2016;128:53-67. Epub 20161004. doi: 10.1016/j.visres.2016.09.010. PubMed PMID: 27668990; PMCID: PMC5079778.
74. Sreenivasan KK, Curtis CE, D'Esposito M. Revisiting the role of persistent neural activity during working memory. Trends in cognitive sciences. 2014;18(2):82-9. Epub 20140114. doi: 10.1016/j.tics.2013.12.001. PubMed PMID: 24439529; PMCID: PMC3964018.
75. Christophel TB, Klink PC, Spitzer B, Roelfsema PR, Haynes JD. The Distributed Nature of Working Memory. Trends in cognitive sciences. 2017;21(2):111-24. Epub 20170104. doi: 10.1016/j.tics.2016.12.007. PubMed PMID: 28063661.
76. Fiebelkorn IC, Snyder AC, Mercier MR, Butler JS, Molholm S, Foxe JJ. Cortical cross-frequency coupling predicts perceptual outcomes. NeuroImage. 2013;69:126-37. doi: 10.1016/j.neuroimage.2012.11.021. PubMed PMID: 23186917; PMCID: 3872821.
77. Fiebelkorn IC, Pinsk MA, Kastner S. The mediodorsal pulvinar coordinates the macaque fronto-parietal network during rhythmic spatial attention. Nature communications. 2019;10(1):215. doi: 10.1038/s41467-018-08151-4. PubMed PMID: 30644391.
78. Maris E, Oostenveld R. Nonparametric statistical testing of EEG- and MEG-data. Journal of neuroscience methods. 2007;164(1):177-90. Epub 20070410. doi: 10.1016/j.jneumeth.2007.03.024. PubMed PMID: 17517438.
79. Bosman CA, Womelsdorf T, Desimone R, Fries P. A microsaccadic rhythm modulates gamma-band synchronization and behavior. The Journal of neuroscience : the official journal of the Society for Neuroscience. 2009;29(30):9471-80. doi: 10.1523/JNEUROSCI.1193-09.2009. PubMed PMID: 19641110.
80. VanRullen R. How to Evaluate Phase Differences between Trial Groups in Ongoing Electrophysiological Signals. Frontiers in neuroscience. 2016;10:426. Epub 20160914. doi: 10.3389/fnins.2016.00426. PubMed PMID: 27683543; PMCID: PMC5021700.
81. Jeffreys DA, Axford JG. Source locations of pattern-specific components of human visual evoked potentials. I. Component of striate cortical origin. Experimental brain research. 1972;16(1):1-21. doi: 10.1007/BF00233371. PubMed PMID: 4646539.
82. Mendoza-Halliday D, Xu H, Azevedo FAC, Desimone R. Dissociable neuronal substrates of visual feature attention and working memory. Neuron. 2024;112(5):850-63 e6. Epub 20240115. doi: 10.1016/j.neuron.2023.12.007. PubMed PMID: 38228138; PMCID: PMC10939754.
83. Senoussi M, Moreland JC, Busch NA, Dugue L. Attention explores space periodically at the theta frequency. Journal of vision. 2019;19(5):22. doi: 10.1167/19.5.22. PubMed PMID: 31121012.
84. Gresch D, Boettcher SEP, van Ede F, Nobre AC. Shifting attention between perception and working memory. Cognition. 2024;245:105731. Epub 20240125. doi: 10.1016/j.cognition.2024.105731. PubMed PMID: 38278040.
85. Gresch D, Boettcher SEP, Gohil C, van Ede F, Nobre AC. Neural dynamics of shifting attention between perception and working-memory contents. Proceedings of the National Academy of Sciences of the United States of America. 2024;121(47):e2406061121. Epub 20241113. doi: 10.1073/pnas.2406061121. PubMed PMID: 39536078.
86. Worden MS, Foxe JJ, Wang N, Simpson GV. Anticipatory biasing of visuospatial attention indexed by retinotopically specific alpha-band electroencephalography increases over occipital cortex. The Journal of neuroscience : the official journal of the Society for Neuroscience. 2000;20(6):RC63. doi: 10.1523/JNEUROSCI.20-06-j0002.2000. PubMed PMID: 10704517.
87. Harrison SA, Tong F. Decoding reveals the contents of visual working memory in early visual areas. Nature. 2009;458(7238):632-5. Epub 20090218. doi: 10.1038/nature07832. PubMed PMID: 19225460; PMCID: PMC2709809.

88. Serences JT, Ester EF, Vogel EK, Awh E. Stimulus-specific delay activity in human primary visual cortex. Psychological science. 2009;20(2):207-14. Epub 20090108. doi: 10.1111/j.1467-9280.2009.02276.x. PubMed PMID: 19170936; PMCID: PMC2875116.
89. Ester EF, Serences JT, Awh E. Spatially global representations in human primary visual cortex during working memory maintenance. The Journal of neuroscience : the official journal of the Society for Neuroscience. 2009;29(48):15258-65. doi: 10.1523/JNEUROSCI.4388-09.2009. PubMed PMID: 19955378; PMCID: PMC2830793.
90. Christophel TB, Hebart MN, Haynes JD. Decoding the contents of visual short-term memory from human visual and parietal cortex. The Journal of neuroscience : the official journal of the Society for Neuroscience. 2012;32(38):12983-9. doi: 10.1523/JNEUROSCI.0184-12.2012. PubMed PMID: 22993415; PMCID: PMC6621473.
91. Gresch D, Boettcher SEP, van Ede F, Nobre AC. Shielding working-memory representations from temporally predictable external interference. Cognition. 2021;217:104915. Epub 20210929. doi: 10.1016/j.cognition.2021.104915. PubMed PMID: 34600356; PMCID: PMC8543071.
92. Bancroft TD, Hockley WE, Servos P. Does stimulus complexity determine whether working memory storage relies on prefrontal or sensory cortex? Attention, perception & psychophysics. 2014;76(7):1954-61. doi: 10.3758/s13414-013-0604-0. PubMed PMID: 24452382.
93. Verschooren S, Pourtois G, Egner T. More efficient shielding for internal than external attention? Evidence from asymmetrical switch costs. Journal of experimental psychology Human perception and performance. 2020;46(9):912-25. Epub 20200507. doi: 10.1037/xhp0000758. PubMed PMID: 32378935.
94. Hautekiet C, Verschooren S, Langerock N, Vergauwe E. Attentional switching between perception and memory: Examining asymmetrical switch costs. Attention, perception & psychophysics. 2023;85(5):1398-408. Epub 20230228. doi: 10.3758/s13414-023-02665-w. PubMed PMID: 36854926; PMCID: PMC10372125.
95. Oostenveld R, Fries P, Maris E, Schoffelen JM. FieldTrip: Open source software for advanced analysis of MEG, EEG, and invasive electrophysiological data. Computational intelligence and neuroscience. 2011;2011:156869. doi: 10.1155/2011/156869. PubMed PMID: 21253357; PMCID: 3021840.
96. Perrin F, Pernier J, Bertrand O, Giard MH, Echallier JF. Mapping of scalp potentials by surface spline interpolation. Electroencephalography and clinical neurophysiology. 1987;66(1):75-81. doi: 10.1016/0013-4694(87)90141-6. PubMed PMID: 2431869.